Mutations in the Histone Methyltransferase Gene, *KMT2B* Cause Early Onset Dystonia

[1]Meyer E^, [2,3]Carss KJ^, [4]Rankin J^, [5]Nichols J, [6,7]Grozeva D, [8]Joseph AP, [9]Mencacci NE, [1,10]Papandreou A, [1,10]Ng J, [1]Barral S, [1,10]Ngoh A,[11]Ben-Pazi H, [12]Willemsen MA, [13]Arkadir D, [14] Barnicoat A,[15]Bergman H, [10]Bhate S, [16]Boys A, [17]Darin N, [18]Foulds N, [19]Gutowski N, [20]Hills A, [9]Houlden H, [14]Hurst J, [21]Israel Z, [22]Kaminska M, [23]Limousin P, [22]Lumsden D, [24]McKee S, [25,26]Misra S, [25,26]Mohammed SS, [22]Nakou V, [27]Nicolai J, [28]Nilsson M, [29]Pall H, [30]Peall KJ, [31]Peters GB, [10]Prabhakar P, [32]Reuter MS, [33]Rump P, [34]Segel R, [27]Sinnema M, [35]Smith M, [4]Turnpenny P, [15]White S, [36]Wieczorek D, [20]Wilson B, [14]Winter G, [19]Wragg C, [37]Pope S, [37,38]Heales SJH, [39]Morrogh D, [7]The UK10K Consortium, [40]DDD study, [3]NIHR Bioresource Rare Diseases Consortium, [9]Pittman A, [10]Carr LJ, [41,42]Perez-Dueñas B, [22]Lin JP, [32]Reis A, [43]Gahl WA, [43]Toro C, [9,23]Bhatia KB, [9,23]Wood NW, [44]Kamsteeg EJ, [45]Chong WK, [5]Gissen P, [8]Topf M, [25,26]Dale RC, [5]Chubb JR, [3,6,7]Raymond FL+, [1,10]Kurian MA+ *

^These authors contributed equally

+These authors contributed equally

*Corresponding author**: Dr Manju Kurian** (manju.kurian@ucl.ac.uk)

Affiliations:

1. Molecular Neurosciences, Developmental Neurosciences, UCL-Institute of Child Health, London, UK

2. Department of Haematology, University of Cambridge, NHS Blood and Transplant Centre, Cambridge, UK
3. NIHR Bioresource Rare Diseases, University of Cambridge, Cambridge, UK
4. Clinical Genetics, Royal Devon & Exeter Hospital, Exeter, UK
5. MRC Laboratory for Molecular Cell Biology, UCL, London, UK
6. Department of Medical Genetics, Cambridge Institute for Medical Research, University of Cambridge, Cambridge, UK
7. Wellcome Trust Sanger Institute, Hinxton, Cambridge, UK
8. Institute of Structural and Molecular Biology, Crystallography/Department of Biological Sciences, Birkbeck College, University of London, London, UK
9. Department of Molecular Neuroscience, UCL-Institute of Neurology, London, UK
10. Department of Neurology, Great Ormond Street Hospital, London, UK
11. Pediatric Neurology and Development, Shaare-Zedek Hospital, Jerusalem, Israel
12. Department of Paediatric Neurology, Donders Centre for Brain, Cognition, and Behavior, Radboud University Medical Center, Nijmegen, Netherlands
13. Department of Neurology, Hadassah Medical Center and the Hebrew University, Jerusalem, Israel
14. Department of Clinical Genetics, Great Ormond Street Hospital, London, UK
15. Department of Neurobiology and Neurosurgery, The Hebrew University, Hadassah Medical Centre, Jerusalem, Israel
16. Victoria Clinical Genetics Services, Murdoch Children's Research Institute, Parkville, Victoria, Australia

17. Department of Neurology, The Queen Silvia Children´s Hospital, Sahlgrenska University Hospital, Gothenburg, Sweden
18. Department of Clinical Genetics, Southampton General Hospital, Southampton, UK
19. Department of Neurology, Royal Devon and Exeter NHS Foundation Trust, Exeter, UK
20. Bristol Genetics Laboratory, Bristol, UK
21. Functional and Restorative Neurosurgery, Hadassah University Hospital, Jerusalem, Israel
22. Complex Motor Disorders Service, Evelina Children's Hospital, Guy's & St Thomas' NHS Foundation Trust, London, UK
23. Sobell Department of Motor Neuroscience and Movement Disorders, National Hospital for Neurology and Neurosurgery, London, UK
24. Northern Ireland Regional Genetics Service, Belfast City Hospital, Belfast, UK
25. Child and Adolescent Health, University of Sydney, Sydney, Australia
26. Institute for Neuroscience and Muscle Research, The Children's Hospital at Westmead, University of Sydney, Sydney, Australia
27. Department of Neurology, Maastricht University Medical Center, Netherlands
28. Department of Pediatrics, Piteå Hospital & Umeå University Hospital, Sweden
29. College of Medicine and Dental Studies, The University of Birmingham, Birmingham, UK

30. Neuroscience and Mental Health Research Institute, Institute of Psychological Medicine and Clinical Neurosciences, Cardiff University, Cardiff, UK
31. Department of Cytogenetics, The Children's Hospital at Westmead, Westmead, Australia
32. Institute of Human Genetics, Friedrich-Alexander-Universität Erlangen-Nürnberg, Erlangen, Germany
33. Department of Genetics, University of Groningen, University Medical Center Groningen, Netherlands
34. Medical Genetics Institute and Pediatrics, Shaare Zedek Medical Center and the Hebrew University School of Medicine, Jerusalem, Israel
35. Department of Paediatric Neurology, John Radcliffe Hospital, Oxford, UK
36. Institute of Human Genetics, University Duisburg-Essen, Essen, Germany
37. Neurometabolic Unit, National Hospital for Neurology and Neurosurgery, Queen Square, London, UK
38. Clinical Chemistry, Great Ormond Street Children's Hospital, NHS Foundation Trust, London, UK
39. North East Thames Regional Genetics Service, Great Ormond Street Hospital, London, UK
40. DDD Study, Wellcome Trust Sanger Institute, Hinxton, Cambridge, UK
41. Department of Child Neurology, Hospital Sant Joan de Déu, Universitat de Barcelona, Barcelona, Spain
42. Centre for Biomedical Research in Rare Diseases (CIBERER-ISCIII), Hospital Sant Joan de Déu, Barcelona, Spain
43. NIH Undiagnosed Diseases Program, Common Fund, Office of the Director,

National Institutes of Health, Bethesda, Maryland, USA

44. Department of Human Genetics, Radboud University Medical Center, Nijmegen, Netherlands

45. Department of Radiology, Great Ormond Street Hospital, London, UK

ABSTRACT

Histone lysine methylation mediated by mixed-lineage leukemia (MLL) proteins, has emerged as critical in the regulation of gene expression, genomic stability, cell cycle and nuclear architecture. Although postulated to be essential for normal development, little is known about the specific functions of the different MLL lysine methyltransferases. Here, we report heterozygous mutations in *KMT2B (MLL4*) in 27 unrelated individuals with a complex progressive childhood-onset dystonia, often associated with a typical facial appearance and characteristic findings on brain magnetic resonance imaging. Over time the majority developed prominent cervical, cranial and laryngeal dystonia. Marked clinical benefit was observed following deep brain stimulation (DBS), leading to even restoration of independent ambulation in some cases. Decreased gene expression of *THAP1* and *TOR1A* was evident in cultured skin fibroblasts from subjects with *KMT2B* mutations, with reduced THAP1 protein levels on immunoblotting. Analysis of cerebrospinal fluid from *KMT2B* mutation-positive patients revealed markedly reduced levels of dopamine 2 receptor protein, with increased tyrosine hydroxylase levels. Our findings highlight a major new, clinically recognizable, and potentially treatable form of genetic dystonia, demonstrating the crucial role of KMT2B in the physiological control of voluntary movement.

INTRODUCTION

The control of voluntary movement is governed by interactive neural networks within the brain, involving the basal ganglia, sensorimotor cortex, cerebellum and thalamus[1]. Disruption of such pathways can lead to the development of a variety of motor disorders. Dystonia is one such movement disorder characterized by sustained or intermittent muscle contractions, causing abnormal, often repetitive movements and postures affecting the limbs, trunk, neck and face. Dystonic movements are typically patterned, twisting, and may be tremulous, often initiated or worsened by voluntary action and associated with overflow muscle activation[2].

Dystonia is the 3rd most commonly reported movement disorder worldwide[1]. It is described in a broad spectrum of genetic and acquired disorders, either in isolation or combined with other neurological and systemic features[2]. The precise pathophysiological processes remain yet to be fully elucidated, but defective dopaminergic signaling is thought to play an important role in many forms of isolated and complex dystonia[1,3-5].

Despite genetic advances, the underlying cause remains elusive for a significant proportion of individuals with childhood-onset dystonia, hindering future prognostication and treatment strategies[6]. Here we report 27 individuals with an early-onset, complex, combined progressive dystonia associated with mono-allelic mutations in *KMT2B* (*MLL4*, OMIM *606834). *KMT2B* encodes a lysine histone methyltransferase, involved in H3K4 methylation, an important epigenetic modification associated with active gene transcription.

RESULTS

Chromosomal microdeletions and intragenic KMT2B mutations in early-onset dystonia

We identified a cohort of 34 patients with undiagnosed childhood-onset dystonia for further molecular genetic investigation ([**Online Methods, Supplementary Table 1**, **Supplementary Fig. 1**). On routine diagnostic testing, one case (Patient 1) was found to have a microdeletion at 19q13.12 of undetermined significance[7]. Diagnostic chromosomal microarray was therefore undertaken in as many patients as logistically possible from this cohort (n=20) and overlapping microdeletions were detected in 5 more children (**Supplementary Table 1**, Patients 2-6). Using established networks (**Online Methods, Supplementary Fig. 1**), 4 more cases (Patients 7-10) with microdeletions were identified. In total, 10 patients (Patients 1-10) were found to have overlapping heterozygous interstitial microdeletions at 19q13.11-19q13.12 (**Table 1a, Fig.1**). Deletions detected on diagnostic microarray studies were confirmed by standard established laboratory protocols and confirmed *de novo* where parental testing was possible (**Supplementary Table 2a**). The smallest region of overlap extended from 36,191,100-36,229,548bp (GRCh37/Hg19), and contained two HUGO Gene Nomenclature Committee curated genes, *ZBTB32* (zinc finger and BTB domain containing 32) and *KMT2B* (*MLL4*) (**Fig. 1**).

Of the remaining 28 patients from the original cohort, we undertook research exome (n=6) and genome sequencing (n=9) in 15 patients (**Online Methods**). Heterozygous variants of *KMT2B* were identified in 6/15 cases (Patients 13, 14, 17,

21, 22, 27). Subsequent Sanger sequencing of *KMT2B* in the other 13/28 individuals from the original cohort detected one more mutation-positive case (Patient 16). A further 10 cases (Patients 11, 12, 15, 18, 19, 20, 23, 24, 25, 26a) were ascertained through both national and international collaborators (**Online Methods, Supplementary Fig. 1**). In total, 17 patients with intragenic heterozygous *KMT2B* variants were identified, harboring frameshift insertions (n=1), frameshift deletions (n=6), splice site (n=1), stop-gain (n=2) and missense (n=7) mutations (**Fig.1**). All *KMT2B* mutations were confirmed on Sanger sequencing and parental segregation studies completed where DNA was available (**Table 1a, Fig. 1, Supplementary Table 2a, Supplementary Fig. 2**). No pathogenic variants in either *ZBTB32* or other known disease-associated genes (including genes causing clinically similar forms of dystonia) were otherwise identified in patients who had whole exome or genome sequencing. In the remaining patients, where further genetic testing was possible, mutations in *TOR1A, THAP1 and GNAL* were excluded by diagnostic single gene testing, multiple gene panel testing or research Sanger sequencing (**Supplementary Table 3**).

Phenotypic characterization of patients with KMT2B mutations

Overall, we identified 27 patients (current age 6-40 years, 14 female, 13 male) with childhood-onset progressive dystonia (**Table 1a, Table 1b, Supplementary Table 4, Supplementary Videos 1-7**). Individuals presented in early childhood (1-9 years, median age 4 years) with either limb or cranio-cervical dystonia. Clinical presentation for those with microdeletions, frameshift, splice-site and stop-gain variants (mean age 4.1 years) occured significantly earlier than for those with intragenic missense mutations (mean age 6.4 years) (p-value 0.0223)

(**Supplementary Fig. 3a**). Most patients (21/27) had lower limb symptoms at disease onset, leading to foot posturing, toe-walking and gait disturbance (**Fig. 2a**). 4/27 patients presented initially with upper limb symptoms associated with abnormal postures (**Fig. 2b,c**) and dystonic tremor, leading to reduced dexterity and handwriting difficulties (**Supplementary Fig. 4a,b**). With increasing age, cervical symptoms (torticollis, retrocollis) (**Fig. 2d,e**) and cranial involvement (facial dystonia, oromandibular involvement with dysarthria/anarthria and difficulties in chewing/swallowing) became prominent features in the majority of patients. In many patients, progressively severe dysphonia was suggestive of laryngeal involvement. None of the patients had airway compromise and videostroboscopy was not undertaken. Over time, the majority of patients (24/27) developed progressive generalized dystonia, 2-11 years after initial presentation (**Fig. 2f**). The dystonia was persistent in nature, absent in sleep, worsened by voluntary action and associated with overflow muscle activation. Some patients had dystonic tremor. Sudden, brief, involuntary muscle jerks, clinically consistent with myoclonus was evident in 2 cases (Patients 14 and 27). For a few subjects, dystonia was exacerbated when systemically unwell. Stepwise deterioration following intercurrent illness was particularly evident in Patient 14, and status dystonicus, triggered by a urinary tract infection, was reported in Patient 3.

Many patients with *KMT2B* mutations had further clinical findings. Additional neurological symptoms and signs were evident in some patients, including microcephaly, seizures, spasticity and eye movement abnormalities (strabismus, saccade initiation failure and oculomotor apraxia) (**Table 1b**). Dysmorphic features and characteristic facial appearance (elongated face and bulbous nasal tip) (**Fig. 2g, Table 1b**) were commonly reported. Delay in neurodevelopmental milestones,

intellectual disability, systemic (dermatological, renal, respiratory) features and psychiatric symptoms were also present in some individuals (**Table 1b, Supplementary Table 4, Supplementary Fig. 4c**). Malignancies were not reported in any patients. Cerebrospinal fluid (CSF) neurotransmitter analysis was undertaken in 13 patients revealing no major derangement of monoamine metabolites (**Supplementary Table 5a**). Magnetic resonance (MR) imaging revealed a characteristic signature in 17/22 patients who had imaging sequences suitable for assessment (**Supplementary Table 5b**). Subtle symmetrical hypointensity of the globus pallidi (with a hypointense streak of bilateral globus pallidus externa) was evident on MR images known to be sensitive to the magnetic resonance phenomenon of susceptibility (T2*-, susceptibility- and echo-planar imaging b0-diffusion-imaging datasets) (**Fig. 3**)**.** The mean age at neuroimaging was significantly lower for patients with MR abnormalities (11.7 years) than for those with normal brain scans (19.0 years) (p-value 0.0167) (**Supplementary Fig. 3b**). Single positron emission tomography using ^{123}I (DaTSCAN^{TM}) and 18 FDG-PET-CT glucose uptake studies, each undertaken in 3 patients, were normal (**Supplementary Table 5b, Supplementary Fig. 4d**).

Deep brain stimulation: clinical benefit in KMT2B-dystonia

Overall, medical therapies were not of clinical benefit in this patient cohort. None of the patients had a sustained response to levodopa treatment, nor other commonly used anti-dystonic agents (**Table 1a**). Due to the medically intractable, progressive nature of disease, 10 patients had symptomatic treatment with bilateral globus pallidus interna-deep brain stimulation (GPi-DBS) (**Table 1a**). All showed clinical benefit with DBS (which was particularly striking in some of the younger patients)

with overall amelioration of dystonia, improved oromandibular symptoms, better upper and lower limb function and even restoration of independent ambulation in some patients. Patient 6 showed significant improvement of torticollis and retrocollis, as well as in overall function and gait after DBS. Patient 8 showed a sustained clinical response 6 years after DBS insertion, with improvement of dystonia, even more evident after replacement of a faulty right DBS lead. Patient 9 had generalized dystonia and could not walk independently pre-DBS. Two weeks post-DBS insertion he dramatically regained independent ambulation with marked improvement of dystonic symptoms (**Supplementary Video 8**). Patient 17 and 21 were predominantly wheelchair-dependent pre-DBS insertion, but both patients showed restoration of independent walking and improvement of dystonia after DBS (**Supplementary Video 9,10**). Patient 19 had improvement in oromandibular symptoms with DBS. Patient 20 had DBS insertion at age 32 years and although most benefits were only transient, sustained improvement of foot posture was reported. Patient 23 had significant amelioration of dystonia symptoms after DBS insertion. Patient 22, now 9 months post-DBS (**Supplementary Video 11**) and Patient 25, 4 months post-DBS have both shown significant gains in hand function and independent walking with reduction of dystonia. Five patients in the cohort are now over three years post-surgery, and the observed reduction of dystonia, restoration of function and prevention of progressive disability is evidence of sustained clinical benefit.

KMT2B is constrained for missense and predicted protein truncating variants

Four individuals (Patient 13, 14, 17 and 21) had whole genome sequencing as part of the NIHR-funded BioResource-Rare Disease project. Enrichment analysis was undertaken in this cohort in order to determine whether predicted protein truncating

variants (PPTVs) in *KMT2B* are observed more frequently in patients than would be expected by chance. Given the size and sequence context of *KMT2B*, $5.73x10^{-03}$ *de novo* PPTVs are expected to occur by chance in *KMT2B* in the subset of the NIHR BioResource- Rare Diseases cohort who have pediatric onset neurological disease, but 3 PPTVs are observed. This represents a significant enrichment (p-value $3.12x10^{-08}$). Furthermore in ExAC, *KMT2B* is also highly constrained for PPTVs. In the ExAC database of 60,706 individuals (Exome Aggregation Consortium (ExAC), Cambridge, MA (URL: http://exac.broadinstitute.org, accessed July 2016)[8], there are only 5 PPTVs that are not flagged as having dubious variant annotation. All are extremely rare (4 are found in a single individual and one occurs in 2 individuals). Given the size and sequence context of the gene, the presence of so few PPTVs in a cohort of 60,706 individuals reveals *KMT2B* to be highly constrained for such variation, providing supportive evidence of its pathogenicity. Regarding variants in the ExAC database, there are 712 reported non-synonymous changes. Most of these are rare, as expected for a cohort of this size, and the median CADD score[9] for these variants is 22.9. The median CADD score for missense mutations identified in our KMT2B-dystonia cohort is significantly higher at 29.1 (p-value 0.0001364; **Supplementary Table 2b**). Furthermore, given the size and sequence context of *KMT2B*, 956 missense variants are predicted to occur by chance, suggesting that *KMT2B* may also be constrained for missense variation (z=4.06)[8].

KMT2B variants are predicted to destabilize protein structure

In silico homology modelling studies were undertaken to generate hypotheses regarding the predicted effects of mutations on KMT2B structure-function properties (**Supplementary Results**). Based on Pfam domain assignments, KMT2B has a

CXXC zinc finger domain, multiple PHD domains, an F/Y rich N-terminus (FYRN), FYRC (F/Y rich N-terminus) domain and a C-terminal SET domain (**Fig. 4a**). The modelled mutations occurred in residues within the PHD-like, FYRN, SET and FYRC-SET linking domains (**Fig. 4b-d**). Evaluation of a number of mutations using MAESTRO[10] and DUET[11] suggests change in free energy, with a predicted structure destabilizing effect (**Supplementary Results**).

Mutations Phe1662Leu and Gly1652Asp occur within a PHD-like domain (residues 1574-1688), predicted to facilitate interaction with DNA, protein-protein interaction and recognition of methylated/unmethylated lysines[12-14]. Extensive hydrophobic interactions hold the globular structure of this region, which is important for its function[12]. Phe1662 is fully buried at the core, stabilizing the structure of this PHD-like domain while Gly1652 is partially buried (**Fig. 4b,e,f**). Phe1662 is involved in multiple hydrophobic contacts at the core of the PHD domain, and mutation to leucine is predicted to cause loss of contacts at the core (**Fig. 4g**). Gly1652 is located on a loop (**Fig. 4e**) and mutation to aspartic acid is predicted to alter surface charge, with possible effect on the interaction network in the vicinity, involving a positively charged Arg1635, part of the helix α3 implicated in DNA binding[12]. Arg1762 and Leu1781 occur in a FYRN domain. FYRN and FYRC regions, particularly common in MLL histone methyltransferases, interact to form a compact structural unit (**Fig. 4c,h**), important in maintaining the active structure[15,16]. Arg1762 forms hydrogen bonds with the backbone carboxyls of Arg2463 and Leu2464 of FYRC domain. Substitution of Arg1762 by cysteine is predicted to abolish these contacts and hence contribute to destabilization of FYRC-FYRN association. Leu1781, at the interface between FYRN and FYRC (**Fig. 4h,i**) is surface exposed and involved in backbone hydrogen bonds stabilizing the beta sheet formed

together by the two domains. Mutation to proline is predicted to disrupt the backbone hydrogen bond at this position, because it lacks one hydrogen bond donor and its backbone torsion angles are not compatible with that of a beta sheet, with a predicted destabilizing effect on sheet structure, potentially affecting the normal association of FYRN and FYRC domains. Arg2517 resides in the region linking FYRC and SET domains, known to bind WDR5, an effector required for trimethylation of histone H3[17], presenting methylated histone H3 substrates to the MLL complex for further methylation[18]. Arg2517 is thought to be involved in a salt-bridge interaction with Asp172 of WDR5 (**Fig. 4j**) and Arg2517Trp is predicted to lead to loss of this interaction. Ile2674, Tyr2688 and Ile2694 occur in the catalytic methyltransferase SET domain common to histone lysine methyltransferases. Ile2674 is buried in the hydrophobic core, adjacent to the catalytic site (**Fig. 4d,k**). Mutation to threonine is predicted to lead to loss of contacts at the core of the domain (due to the shorter side chain) and also introduces a buried polar group (**Fig. 4k,l**). Tyr2688Thr occurs at the core of SET domain involving extensive hydrophobic interactions and a hydrogen bond interaction with Ser2661 (**Fig 4m**). The frameshift mutation Tyr2688Thrfs*50 with insertion of 50 additional residues, is predicted to destabilise the core and affect contacts due to the substitution with a shorter non-aromatic side-chain. Ile2694 is involved in the extensive hydrophobic contacts stabilizing the core of this domain. *In silico* analysis predicts that the frameshift mutation Ile2694Serfs*44 will disrupt the domain fold and affect methytransferase activity.

KMT2B is ubiquitously expressed with reduced expression in KMT2B-dystonia

We confirmed widespread *KMT2B* expression in a variety of control fetal and adult human tissues (**Fig. 5a**). Moreover, *KMT2B* is ubiquitously expressed in the brain, with higher expression in the cerebellum than any other region (**Fig. 5b**). We ascertained fibroblasts from 4 patients (Patient 2, 13, 14, 16, with either microdeletions or PPTVs in *KMT2B*) and detected a statistically significant decrease in fibroblast *KMT2B* expression on quantitative RT-PCR when compared to control fibroblasts (**Fig. 5c**).

Histone H3K4 methylation is not globally reduced in KMT2B-dystonia

To determine the effect of *KMT2B* mutations on methylation of lysine 4 on histone H3 (H3K4 methylation), we assayed tri-methylated H3K4 (H3K4me3) and di-methylated H3K4 (H3K4me2). Immunoblotting of histones extracted from fibroblasts of Patient 14 and 16 showed no significant reduction in H3K4me3 or H3K4me2 relative to control samples (**Fig. 5d, Supplementary Fig. S5a**). We used the model species *Dictyostelium discoideum* to test the effect of SET domain mutation Ile2647Thr on *in vivo* histone methyltransferase activity. The SET domain of KMT2B shares 56**%** sequence identity with the *Dictyostelium* orthologue DdSet1, and Ile2647 is conserved (corresponding amino acid in *Dictyostelium* is Ile1447) (**Fig. 1h**). DdSet1 is the only H3K4 methyltransferase in *Dictyostelium* and targeted knockout of *DdSet1* (*set1*$^{-}$) results in loss of all methylation at H3K4[19]. We constitutively expressed wild-type DdSet1 (WT-DdSet1) and mutant-DdSet1 (m-DdSet1), both with N-terminal GFP fusions, in *set1- Dictyostelium* cells and compared the resulting levels of H3K4 methylation. Expression of either GFP-WT-DdSet1 or GFP-mDdSet1 in *set1-* cells resulted in rescue of H3K4 tri-methylation to wild type levels (**Fig. 5e, Supplementary Fig. S5b, S5c**).

364 ***Fibroblast THAP1 gene and protein expression is reduced in KMT2B-dystonia***

365 In order to determine whether KMT2B-dystonia is associated with dysregulation of
366 specific genes implicated in the control of movement, we investigated the
367 expression profiles of *TOR1A* and *THAP1.* Fibroblasts derived from 4 patients
368 (Patients 2, 13, 14, 16) showed significantly reduced transcript levels of *THAP1* and
369 *TOR1A* when compared to control fibroblasts (**Fig. 5f**). Fibroblast immunoblotting
370 studies showed a statistically significant reduction in THAP1 protein expression in
371 all 4 patients when compared to control samples (**Fig. 5g**). A statistically significant
372 reduction in TOR1A protein level was evident in Patient 14, though not in the other
373 patients (**Fig. 5h**).

374 ***Abnormal CSF levels of dopaminergic proteins in KMT2B-dystonia***

375 CSF immunoblotting studies were undertaken in two patients for whom samples
376 were available for research testing (Patient 2 and 16). Both patients had markedly
377 reduced levels of dopamine 2 receptor (D2R), 56.9% and 59.8% of levels observed
378 in control CSF (Controls = 1.09±0.21SD, KMT2B patients = 0.64±0.02SD). In
379 contrast, an increase in tyrosine hydroxylase (TH) levels was seen in both mutation-
380 positive patients (173.3% and 170.9% of levels seen in control CSF) (Controls =
381 0.52±0.08SD, KMT2B patients = 0.90±0.01SD) (**Fig. 5i**).

382 ## DISCUSSION

383 We report 27 individuals with heterozygous mutations in the lysine
384 methyltransferase gene, *KMT2B,* and define a new genetic movement disorder that
385 importantly, is amenable to treatment with DBS. Using the current classification
386 system[2], KMT2B-dystonia is defined as an inherited autosomal dominant, complex,

combined dystonia usually of infantile or childhood-onset. In most patients, the dystonia is persistent and progressive in nature. The majority of individuals develop 4-limb dystonia with particularly prominent cervical, laryngeal and oromandibular symptoms. Whilst the majority of patients in this cohort seem to follow this disease trajectory, we also report atypical cases with relatively little limb involvement and either mainly oromanibular features (Patient 18) or paroxysmal cervical dystonia (Patient 26a).

For many patients, KMT2B-dystonia is associated with a number of additional clinical features, including other neurological symptoms, intellectual disability, psychiatric co-morbidity, dysmorphia, skin lesions and other systemic signs. Given the association with active gene expression, is possible that *KMT2B* could account for these additional disease features. For Patients 1-10, is also possible that other genes within their microdeletion could contribute to aspects of their clinical phenotype. Indeed, cutis aplasia and ectodermal dysplasia have been reported in patients with more proximal deletions of chromosome 19q13.11[20]. KMT2B is therefore a complex dystonia, and affected patients should have close surveillance of development during childhood, regular neurology assessments, routine dermatological review and formal neuropsychiatric testing.

In KMT2B-dystonia, the majority of patients had a characteristic pattern on MR imaging, with very subtle low pallidal signal on T2*-, diffusion- and susceptibility-weighted sequences, particularly affecting the lateral aspect of the globus pallidus externa (**Fig. 3**). Although genotype did not appear to influence whether MR findings were evident, those with abnormal imaging had scans undertaken at a significantly younger age than those with normal imaging. Indeed, MR abnormalities could possibly be an age-dependent phenomenon, perhaps becoming less

412 apparent with increasing age, as was evident in Patient 22 (**Supplementary Table**
413 **5b, Supplementary Fig. 3b,c,d**). The overall significance of the identified
414 neuroradiological abnormalities remains unclear. Such radiological findings are
415 reminiscent of, but much more subtle and different to those reported in classical
416 Neurodegeneration with Brain Iron Accumulation (NBIA) syndromes[21,22]. Similar
417 non-specific features of T2*-weighted hypointensity are increasingly recognized in a
418 number of other neurological conditions, including Huntington's disease, *TUBB4A*-
419 related disorders, GM1 gangliosidosis, alpha-fucosidosis and
420 mitochondriocytopathies.

421 In the original UCL-ICH Dystonia cohort, *KMT2B* mutations were identified in 13/34
422 (38%) individuals with a relatively homogenous phenotype of early onset
423 progressive dystonia. In other screened cohorts, mutation detection rates varied
424 from 1.3-30%, with more cases identified from cohorts that were tightly phenotyped
425 for dystonia (**Supplementary Fig. 1**). In screened cases where *KMT2B* mutations
426 were not detected, it is likely that these individuals have another underlying etiology
427 accounting for their symptoms, although it is possible that (i) single/multiple exon
428 *KMT2B* deletions and duplications may have been missed on microarray, Sanger
429 sequencing and whole exome/genome sequencing and (ii) promoter mutations and
430 deeply intronic *KMT2B* variants may not have been detected by whole exome and
431 Sanger sequencing.

432 The majority of individuals with *KMT2B* mutations (20/27, Patients 1-20) had either
433 heterozygous interstitial microdeletions leading to *KMT2B* haploinsufficiency, or
434 variants predicted to cause protein truncation, protein elongation, splicing defects or
435 nonsense-mediated mRNA decay. The remaining 7 patients (Patients 21-27) had
436 previously unreported non-synonymous variants of *KMT2B*, all affecting conserved

residues within key protein domains (**Fig. 1c-h**), and *in silico* studies predict destabilization of protein structure. Notably, initial disease presentation was significantly earlier in Patients 1-20 than in those with missense variants (**Supplementary Fig. 3a**). In KMT2B-dystonia, genotype did not however influence the rate of symptom evolution, disease severity or response to DBS.

For the majority of patients, *KMT2B* mutations were confirmed as *de novo* where parental testing could be undertaken. In our cohort, 3 patients had missense mutations that were all maternally inherited (Patient 22, 26a, 27). Given this observation of maternal inheritance, the possibility of imprinting at the disease locus was considered, but deemed unlikely, given (i) *de novo* microdeletions in Patients 2 and 10 occurred on paternally inherited alleles and (ii) there is evidence of bi-allelic expression of *KMT2B* single nucleotide polymorphisms in human tissues, including brain (**Supplementary Fig. S6**). Importantly, whole exome sequence analysis undertaken in Patients 22, 26a and 27 did not identify other rare or *de novo* variants to account for their disease. Interestingly, Patient 26a inherited p.Arg2517Trp from his symptomatic mother (26b) who also had (milder) disease symptoms. She reported gait abnormalities and a progressive inability to run, as well as periodic paroxysmal upper limb and neck dystonia. She also had a bulbous nasal tip, like her son (**Fig. 2g**). In contrast, both mothers of Patients 22 and 27 were clinically examined, and neither had evidence of a motor phenotype, intellectual disability, other neurological features, neuropsychiatric symptoms, facial dysmorphia, skin lesions or other systemic signs. The identification of both symptomatic and asymptomatic carriers suggests that there may be either “apparent’ incomplete penetrance, due to parental mosaicism, or true incomplete disease penetrance, a phenomenon commonly reported in a number of other autosomal dominant genetic

dystonias[23,24]. Furthermore, other genetic, epigenetic and environmental modifiers may also influence disease penetrance and phenotypic presentation in KMT2B-dystonia.

KMT2B encodes an ubiquitously expressed lysine methyltransferase specifically involved in H3K4 methylation[25,26], an important epigenetic modification associated with active transcription. H3K4me3 is enriched at promoters, marking transcription start sites of actively transcribed genes, whereas H3K4me1 is associated with active enhancer sequences[27]. H3K4me2 is less specifically localized, but may be enriched at transcription factor binding sites[28]. Members of the SET/MLL protein family, including KMT2B, are responsible for the generation of H3K4me1, H3K4me2, and H3K4me3, essential for gene activation in normal development[29]. Using patient-derived fibroblasts and a *Dictyostelium discoideum* model, we demonstrated that *KMT2B* mutations are not associated with widespread alterations in overall levels of H3K4 methylation. This is not surprising, given that haploinsufficiency of other MLL family members have not been convincingly shown to affect global H3K4 levels. The fundamental physiological role of MLL proteins is however further affirmed by the observation that loss-of-function heterozygous mutations in MLL-encoding genes are reported in human developmental disorders[30], namely Wiedemann Steiner (*KMT2A, MLL1*)[31], Kleefstra-like (*KMT2C, MLL3*)[32], Kabuki (*KMT2D, MLL2*)[33] syndrome, and most recently *SETD1A*-related disease (*KMT2F*)[34]. The physiological functions of MLL proteins are yet to be fully characterized, however, the observation that mutations in different MLL genes cause phenotypically distinct syndromes (**Supplementary Table 6**) suggests that each MLL protein has a unique role regulating the expression of a specific set of genes[35,36].

Amongst the 4 reported *MLL*-gene disorders, dystonia appears unique to KMT2B-related disease and is not described in other MLL syndromes (**Supplementary Table 6**), providing further evidence that different MLL proteins mediate the activation and transcription of a specific set of genes, with temporal and cellular context[37]. We utilized fibroblasts and CSF derived from patients to investigate downstream effects of *KMT2B* mutations on specific gene expression. The rationale for investigating *THAP1* and *TOR1A* in the first instance was based on a number of factors, namely that (i) loss-of-function mutations in both genes cause progressive generalized dystonia with cervical, oromandibular and laryngeal symptoms, similar to those seen in KMT2B-dystonia[38,39,40], (ii) both genes are expressed in fibroblasts, facilitating investigation in patient-derived tissue, (iii) analysis of methylation profiles using ENCODE demonstrates a sharp H3K4me3 peak at the 5' region of both *THAP1* and *TOR1A* in a wide range of cell types, including brain cells (**Supplementary Fig. 7**), (iv) on human brain expression profiles, *THAP1* and *KMT2B* similarly display highest expression in the cerebellum (**Fig 5b, Supplementary Fig. 8**). We detected statistically significant reduced levels of *THAP1* and *TOR1A* gene expression and THAP1 protein expression in patient fibroblasts. The mechanisms causing such alterations in KMT2B-dystonia remain yet to be elucidated. Whilst H3K4 methylation is clearly associated with the process of active transcription, several studies have shown that H3K4 methylation is required, not for absolute transcriptional output, but rather for transcription stability or consistency[41]. Recent studies have suggested that H3K4Me is required to minimize transcriptional variability between cells in a population, rather than absolute expression[41,42], so the effects of *KMT2B* haploinsufficiency on *THAP1/TOR1A* levels could conceivably operate via an intermediary sensitive to

stochastic fluctuations. Whilst our study focuses on two genes, it is highly likely that dysregulation of other genes and proteins are also involved in the disease pathophysiology of KMT2B-dystonia. Further studies will determine whether expression profiles of other genes are affected in KMT2B-dystonia and contributory to the phenotype.

CSF analysis is increasingly recognized as a highly useful tool for studying synaptic proteins and dysregulation of the dopaminergic system[43]. In our study, CSF immunoblotting studies revealed significant reduction of D2R protein and increase in TH levels in patients with KMT2B-dystonia when compared to control CSF samples. Downregulation of D2R could conceivably impair post-synaptic activation of coupled G-proteins with subsequent downstream effects, as seen in other inherited dystonias. Reduced D2R striatal availability is reported in patients with DYT1 and DYT6 dystonia[44,45]. Furthermore, D2R dysfunction is described in murine DYT1 models, where aberrant D2R-mediated responses are associated with reduced D2R protein levels and impaired G-protein activation[46]. The observed rise in CSF TH levels could be secondary to reduced pre-synaptic D2 autoreceptors[47], which could conceivably impact dopamine synthesis and bioavailability. Interestingly patients with KMT2B-dystonia had normal CSF levels of the stable dopamine metabolite, homovanillic acid (HVA), indicating normal dopamine turnover (conversion of dopamine to HVA by monoamine oxidase and catechol-o-methyl transferase). Whilst CSF HVA levels accurately reflect dopamine turnover, they are not always a true indicator of dopamine synthesis and bioavailability. Low CSF HVA levels often correlate with low dopamine levels in patients with inherited disorders of dopamine deficiency such as TH deficiency, aromatic l-amino acid decarboxylase deficiency, and many inherited pterin defects[3]. However HVA levels

537 may also be normal (autosomal dominant GTP cyclohydrolase deficiency) or
538 elevated (Dopamine Transporter Deficiency Syndrome) in diseases known to be
539 associated with dopamine deficiency[3,48]. Normal HVA levels in KMT2B-dystonia
540 may therefore not reflect true dopamine levels. Indeed, the effect of *KMT2B*
541 mutations on dopamine synthesis and bioavailability remain yet to be fully
542 elucidated.

543 In conclusion, we report *KMT2B* mutations in 27 patients with a clinically
544 recognizable, distinct form of dystonia. To date, the underlying etiology is only
545 genetically resolved in a minority of childhood-onset cases of dystonia, which
546 precludes confirmatory diagnosis, accurate disease prognostication and selection of
547 appropriate treatment strategies. We have shown that many patients with molecular
548 confirmation of KMT2B-dystonia have significant, sustained clinical improvement
549 with DBS and referral for DBS assessment should thus be considered for this group
550 of individuals. Identification of additional cases will allow further characterization of
551 the full phenotypic disease spectrum. Our report highlights mutations in *KMT2B* as
552 a new and important cause of early-onset dystonia, emphasizing the crucial role of
553 KMT2B in the control of normal voluntary movement.

References

1. Charlesworth, G., Bhatia, K.P. & Wood, N.W. The genetics of dystonia: new twists in an old tale. *Brain* **136**, 2017-2037 (2013).
2. Albanese, A. *et al.* Phenomenology and classification of dystonia: a consensus update. *Mov. Disord.* **28**, 863-873 (2013).
3. Ng, J., Papandreou, A., Heales, S.J. & Kurian, M.A. Monoamine Neurotransmitter Disorders – clinical advances and future perspectives. *Nat. Rev. Neurol.* **11**, 567-584 (2015).
4. Fuchs, T. *et al.* Mutations in GNAL cause primary torsion dystonia. *Nat. Genet.* **45**, 88-92 (2013).
5. Karimi, M. & Perlmutter J.S. The role of dopamine and dopaminergic pathways in dystonia: insights from neuroimaging. *Tremor Other Hyperkinet. Mov.* **5**, 280 (2015).
6. Lin, J.P., Lumsden, D.E., Gimeno, H. & Kaminska, M. The impact and prognosis for dystonia in childhood including dystonic cerebral palsy: a clinical and demographic tertiary cohort study. *J. Neurol. Neurosurg. Psychiatry* **85**, 1239-1244 (2014).
7. Dale, R.C., Grattan-Smith, P., Nicholson, M. & Peters, G.B. Microdeletions detected using chromosome microarray in children with suspected genetic movement disorders: a single-centre study. *Dev. Med. Child Neurol.* **54**, 618-623 (2012).
8. Lek, M. *et al.* Analysis of protein-coding genetic variation in 60,706 humans. bioRxiv [Internet]; Available from: http://biorxiv.org/content/early/2015/10/30/030338.abstract (2015).
9. Kircher, M. *et al.* A general framework for estimating the relative

579 pathogenicity of human genetic variants. *Nat. Genet.* **46**, 310-315 (2014).
580 10. Laimer, J., Hofer, H., Fritz, M., Wegenkittl, S. & Lackner, P. MAESTRO--
581 multi agent stability prediction upon point mutations. *BMC Bioinformatics* **16**,
582 116 (2015).
583 11. Pires, D.E., Ascher, D.B. & Blundell, T.L. DUET: a server for predicting
584 effects of mutations on protein stability using an integrated computational
585 approach. *Nucleic Acids Res.* **42**, W314-319 (2014).
586 12. Liu, Z. *et al.* Structural and functional insights into the human Borjeson-
587 Forssman-Lehmann syndrome-associated protein PHF6. *J. Biol. Chem.* **289**,
588 10069-10083 (2014).
589 13. Musselman, C.A. & Kutateladze, T.G. Handpicking epigenetic marks with
590 PHD fingers. *Nucleic Acids Res.* **39**, 9061-9071 (2011).
591 14. Sanchez, R. & Zhou, M.M. The PHD finger: a versatile epigenome reader.
592 *Trends Biochem. Sci.* **36**, 364-372 (2011).
593 15. Hsieh, J.J., Ernst, P., Erdjument-Bromage, H., Tempst, P. & Korsmeyer, S.J.
594 Proteolytic cleavage of MLL generates a complex of N- and C-terminal
595 fragments that confers protein stability and subnuclear localization. *Mol. Cell.*
596 *Biol.* **23**, 186-194 (2003).
597 16. Pless, B. *et al.* The heterodimerization domains of MLL-FYRN and FYRC--
598 are potential target structures in t(4;11) leukemia. *Leukemia* **25**, 663-670
599 (2011).
600 17. Wysocka, J. *et al*. WDR5 associates with histone H3 methylated at K4 and is
601 essential for H3 K4 methylation and vertebrate development. *Cell* **121**, 859-
602 872 (2005).
603 18. Song, J.J. & Kingston, R.E. WDR5 interacts with mixed lineage leukemia

(MLL) protein via the histone H3-binding pocket. *J. Biol. Chem.* **283**, 35258-35264 (2008).

19. Chubb, J.R. *et al.* Developmental timing in Dictyostelium is regulated by the Set1 histone methyltransferase. *Dev. Biol.* **292**, 519-532 (2006).
20. Malan, V. *et al.* 19q13. 11 deletion syndrome: a novel clinically recognisable genetic condition identified by array comparative genomic hybridisation. *J. Med. Genet.* **46**, 635-664 (2009).
21. Kruer, M.C. *et al.* Neuroimaging features of neurodegeneration with brain iron accumulation. *AJNR Am. J. Neuroradiol.* **33**, 407-414 (2012).
22. Meyer, E., Kurian, M.A. & Hayflick, S.J. Neurodegeneration with Brain Iron Accumulation: Genetic Diversity and Pathophysiological Mechanisms. *Annu. Rev. Genomics Hum. Genet.* **16**, 257-279 (2015).
23. Ozelius, L. *et al.* SourceGeneReviews® [Internet]. Seattle (WA): University of Washington, Seattle; [updated 2014 Jan 02] (1993-2016).
24. Klein, C. *et al.* SourceGeneReviews® [Internet]. Seattle (WA): University of Washington, Seattle; [updated 2014 May 1] (1993-2016).
25. Kouzarides, T. Chromatin modifications and their function. *Cell* **128**, 693-705 (2007).
26. Black, J.C., Van Rechem, C. & Whetstine, J.R. Histone lysine methylation dynamics: establishment, regulation, and biological impact. *Mol. Cell* **48**, 491-507 (2012).
27. Creyghton, M.P. *et al.* Histone H3K27ac separates active from poised enhancers and predicts developmental state. *Proc. Natl. Acad. Sci. U S A* **107**, 21931-21936 (2010).
28. Wang, Y., Li, X. & Hu, H. H3K4me2 reliably defines transcription factor

629 binding regions in different cells. *Genomics* **103**, 222-228 (2014).
630 29. Shao, G.B. *et al.* Dynamic patterns of histone H3 lysine 4 methyltransferases
631 and demethylases during mouse preimplantation development. *In Vitro Cell*
632 *Dev. Biol. Anim.* **50**, 603-613 (2014).
633 30. Shen, E., Shulha, H., Weng, Z. & Akbarian, S. Regulation of histone H3K4
634 methylation in brain development and disease. *Philos. Trans. R. Soc. Lond.*
635 *B. Biol. Sci.* **369** (2014).
636 31. Jones, W.D. *et al.* De novo mutations in MLL cause Wiedemann-Steiner
637 syndrome. *Am. J. Hum. Genet.* **91**, 358-364 (2012).
638 32. Kleefstra, T. *et al.* Disruption of an EHMT1-associated chromatin-
639 modification module causes intellectual disability. *Am. J. Hum. Genet.* **91**,
640 73-82 (2012).
641 33. Ng, S.B. *et al.* Exome sequencing identifies MLL2 mutations as a cause of
642 Kabuki syndrome. *Nat. Genet.* **42**, 790-793 (2010).
643 34. Singh, T. *et al.* Rare loss-of-function variants in SETD1A are associated with
644 schizophrenia and developmental disorders. *Nat. Neurosci.* **19**, 571-577
645 (2016).
646 35. Micale, L. *et al.* Molecular analysis, pathogenic mechanisms, and
647 readthrough therapy on a large cohort of Kabuki syndrome patients. *Hum.*
648 *Mutat.* **35**, 841-850 (2014).
649 36. Ang, S.Y. *et al.* KMT2D regulates specific programs in heart development via
650 histone H3 lysine 4 di-methylation. *Development* **143**, 810-821 (2016).
651 37. Jakovcevski, M. *et al.* Neuronal Kmt2a/Mll1 histone methyltransferase is
652 essential for prefrontal synaptic plasticity and working memory. *J. Neurosci.*
653 **35**, 5097-5108 (2015).

654 38. Ozelius, L.J. *et al.* The early-onset torsion dystonia gene (DYT1) encodes an
655 ATP-binding protein. *Nat. Genet.* **17**, 40-48 (1997).
656 39. Fuchs, T. *et al.* Mutations in the THAP1 gene are responsible for DYT6
657 primary torsion dystonia. *Nat. Genet.* **41**, 286-288 (2009).
658 40. Bressman, S.B. *et al.* Mutations in THAP1 (DYT6) in early-onset dystonia: a
659 genetic screening study. *Lancet Neurol.* **8**, 441-446 (2009).
660 41. Benayoun BA, *et al.* H3K4me3 breadth is linked to cell identity and
661 transcriptional consistency. *Cell* **158**, 673-688 (2014).
662 42. Muramoto, T., Müller, I., Thomas, G. Melvin, A. & Chubb, J.R. Methylation of
663 H3K4 Is required for inheritance of active transcriptional states. *Curr Biol.* **20**,
664 397-406 (2010).
665 43. Ortez, C. *et al.* Cerebrospinal fluid synaptic proteins as useful biomarkers in
666 tyrosine hydroxylase deficiency. *Mol. Genet. Metab*. **114**, 34-40 (2015).
667 44. Carbon, M. *et al.* Abnormal striatal and thalamic dopamine
668 neurotransmission: genotype-related features of dystonia. *Neurology* **72**,
669 2097-2103 (2009).
670 45. Asanuma, K. *et al.* Decreased striatal D2 receptor binding in non-manifesting
671 carriers of the DYT1 dystonia mutation. *Neurology* **64**, 347-349 (2005).
672 46. Napolitano, F. *et al.* Dopamine D2 receptor dysfunction is rescued by
673 adenosine A2A receptor antagonism in a model of DYT1 dystonia.
674 *Neurobiol. Dis.* **38**, 434-445 (2010).
675 47. Lindgren, N., *et al.* Dopamine D(2) receptors regulate tyrosine hydroxylase
676 activity and phosphorylation at Ser40 in rat striatum. *Eur. J. Neurosci.* **13**,
677 773-780 (2001).

678 48. Wijemanne, S. & Jankovic, J. Dopa-responsive dystonia--clinical and genetic
679 heterogeneity. *Nat. Rev. Neurol.* **11**, 414-424 (2015).
680 49. Trabzuni, D. *et al*. Quality control parameters on a large dataset of regionally
681 dissected human control brains for whole genome expression studies. *J.*
682 *Neurochem.* **119**, 275-282 (2011).

Acknowledgements

We would like to thank all our patients and their families for taking part in this study and encouraging international collaboration to seek out similar cases. Thank you to Dr Karin Tuschl for kindly providing the human cDNA panel, Miho Ishida for kindly providing the fetal cDNA and Dr Lorenzo Bassioni for kindly selecting DaTSCAN images for the Supplementary manuscript. MAK has a Wellcome Intermediate Clinical Fellowship. EM and MAK received funding from Gracious Heart Charity, Rosetrees Trust and Great Ormond Street Hospital Children's Charity. This research was supported by the National Institute for Health Research Biomedical Research Centre at Great Ormond Street Hospital for Children NHS Foundation Trust, University College London, and University of Cambridge and from the NIHR for the Bioresource for Rare Diseases (grant number RG65966). This study makes use of data generated by the DECIPHER community. A full list of centres who contributed to the generation of the data is available from http://decipher.sanger.ac.uk and via email from decipher@sanger.ac.uk Funding for the project was provided by the Wellcome Trust for UK10K (WT091310) and DDD Study. The DDD study presents independent research commissioned by the Health Innovation Challenge Fund [grant number HICF-1009-003] see Nature 2015;519:223-8 or www.ddduk.org/access.html for full acknowledgement. AP has a joint Action Medical Research/ British Paediatric Neurology Association Research Training Fellowship and receives funding from the NBIA Disorders Association and Child Brain Research. DA is supported by the Prusiner-Abramsky Award. KJP has an Academy of Medical Sciences Clinical Starter Grant. BPD received funding from grants 20143130-La Marató de TV3 and PI15/00287-Ministerio Español de Economia y Competitividad. JPL has been supported by a Guy's and St Thomas

Charity New Services and Innovation Grant: G060708; The Dystonia Society (UK): Grants 01/2011 and 07/2013 and an Action Medical Research: AMR - GN2097.

Disclosures

HP has unrestricted support for Educational Activity from Medtronic.

714 **Figure 1**

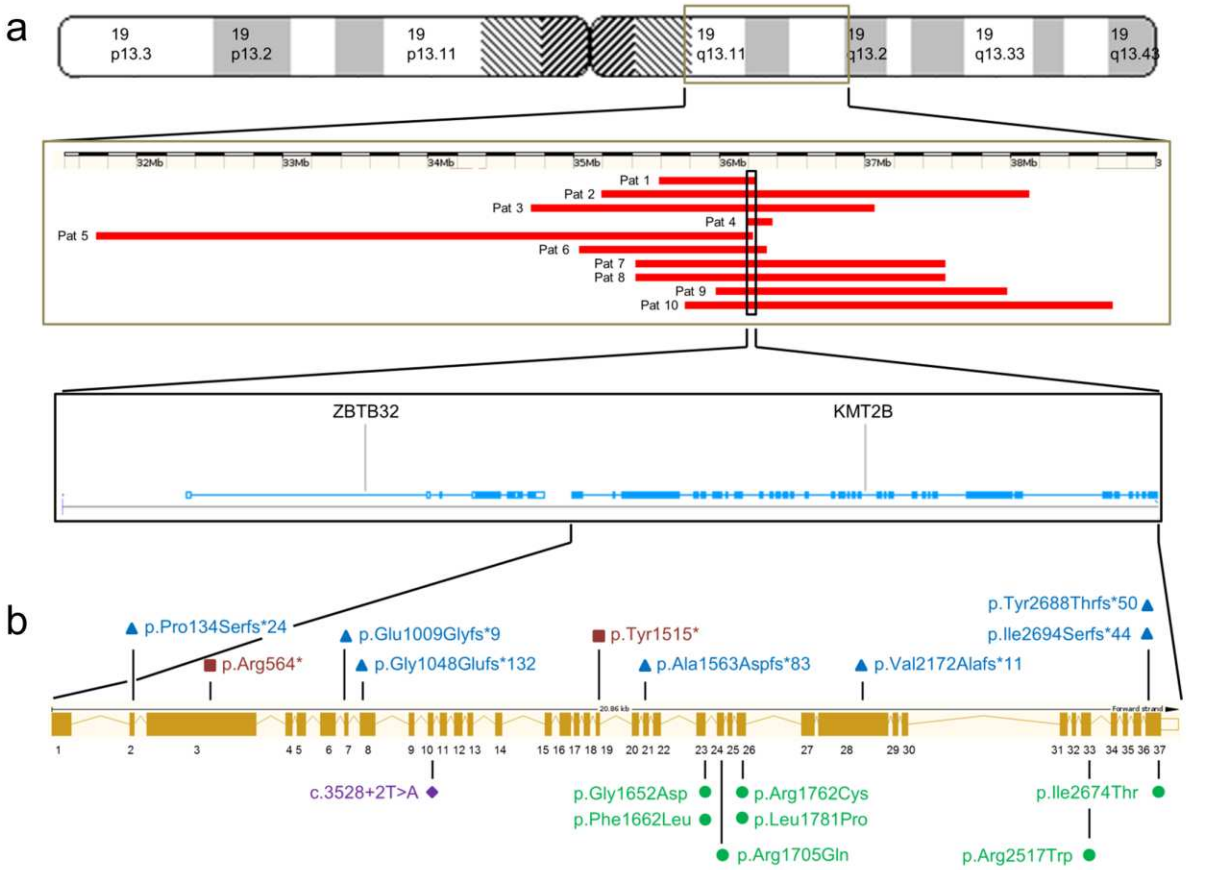

c

```
Human KMT2B        1647 PGATVGCCLSSCLSNFHFMC 1666
Dog KMT2B          1642 PGATVGCCLSSCLSNFHFMC 1661
Cow KMT2B          1642 PGATVGCCLSSCLSNFHFMC 1661
Mouse Kmt2b        1653 PGATVGCCLSSCLSNFHFMC 1672
Zebrafish kmt2ba   1454 TGATVGCCLTSCQSNYHFMC 1473
Zebrafish kmt2bb   2147 TGATVGCCLSSCQSNYHFMC 2166
Fruit fly trx      1803 RGATVGCNVRSCGEHYHYPC 1822
Human KMT2A        1942 PGATVGCCLTSCTSNYHFMC 1961
Human PHF6          286 PGATIGCEIKACVKTYHYHC 305
                        ***:** : :* . :*:
```

d

```
Human KMT2B        1695 VNPDGFDVLRRVYVDFEGIN 1714
Dog KMT2B          1690 VTPDGFDVLRRVYVDFEGIN 1709
Cow KMT2B          1699 VNPDGFDVLRRVYVDFEGIN 1718
Mouse Kmt2B        1701 VTPDGFDVLRRVYVDFEGIN 1720
Zebrafish kmt2ba   1501 EQGNGFEVVRRVYVDFDGIS 1520
Zebrafish kmt2bb   2194 ITGQGFEVLRRVYVDFEGIS 2213
Fruitfly trx       1489 TYESNFEVSRPVYVELD--- 1505
Human KMT2A        1989 VPENGFEVFRRVFVDFEGIS 2008
                          . *:* * *:*:::    **
```

e

```
Human KMT2B        1752 RLFPIGYQCSRLYWSTVDAR 1771
Dog KMT2B          1747 RLFPIGYQCSRLYWSTVDAR 1766
Cow KMT2B          1756 RLFPIGYQCSRLYWSTVDAR 1775
Mouse Kmt2B        1758 RLFPIGYQCSRLYWSTVDAR 1777
Zebrafish kmt2ba   1558 KLYPVGYQCSRWYWSTVDPR 1577
Zebrafish kmt2bb   2251 KLFPVGYECSRWFWSTVNPL 2270
Fruitfly trx       1542 AVVPINFLCSRLYWSSKEPW 1561
Human KMT2A        2046 KLFPIGYQCSRVYWSTTDAR 2065
                          : *: : *** :**: :  :  *
```

f

```
Human KMT2B        1778 CRILEYRPWGPREEPAHLEA 1897
Dog KMT2B          1773 CRILEYRPWGPREEPVHLEA 1792
Cow KMT2B          1773 CRILEYRPWGPREEPVHLEA 1792
Mouse Kmt2b        1784 CRILEYRPWGPREEPVHLEA 1803
Zebrafish kmt2ba   1584 CKVSEVRPSTRCRTPSFMVD 1603
Zebrafish kmt2bb   2277 FRVTEVRPAVQEKQVEESPD 2296
Fruit fly trx      1936 VRTTIQNSSST----LTALD 1951
Human KMT2A        2072 CKIVECRPPVVEPDINSTVE 2091
                           :    .
```

g

```
Human KMT2B        2507 HGAARAEVYLRKCTFDMFNF 2526
Dog KMT2B          2503 HGAARAEVYLRKCTFDMFNF 2522
Cow KMT2B          2512 HGAARAEVYLRKCTFDMFNF 2531
Mouse Kmt2B        2514 HGAARAEVYLRKCTFDMFNF 2533
Zebrafish kmt2ba   2655 NGCARAEVYVRKSTFDMFNF 2674
Zebrafish kmt2bb   3563 SGCARSEVYLRKSTFDMFNF 3582
Fruitfly trx       3155 YDCARCEPYSNRSEYDMFSW 3174
Human KMT2A        3764 HGSARAEVHLRKSAFDMFNF 3783
                          .**.* : .:. :***.:
```

h

```
Human KMT2B        2664 IHVEGQKHIVIFALRRILRG 2783
Dog KMT2B          2660 IHVEGQKHIVIFALRRILRG 2679
Cow KMT2B          2660 IHVEGQKHIVIFALRRILRG 2679
Mouse Kmt2b        2662 IHVEGQKHIVIFALRRILRG 2681
Zebrafish kmt2ba   2812 INVEGQKHIVIFALRKIYRG 2831
Zebrafish kmt2bb   3721 INVEGQKHIVIFALRKIYRG 3740
Fruit fly trx      3677 VDILGHKHIIIFALRRIVQG 3696
Yeast Set1         1028 IKVGGRRRIVIYALRDIAAS 1047
Dicty Set1         1437 LTIGNQKKIIIYAKRDINIG 1456
Human KMT2A        3921 INIDGQKHIVIFAMRKIYRG 3940
Human SETD1A       1658 ITIESQKKIVIYSKQPIGVD 1677
Human SETD1B       1874 ITVESQKKIVIYSKQHINVN 1893
                          : :  :::*:*:: : *
```

715
716

Figure 1:

Molecular Genetics Findings in Patients with *KMT2B* Mutations

(a) Top panel: Schematic representation of chromosome 19. Middle panel: Ten microdeletions on 19q13.11-19q13.12 are displayed as horizontal red bars (GRCh37/Hg19). Lower panel: The smallest overlapping region comprises two genes, *ZBTB32* and *KMT2B*. (**b**) Schematic of exon-intron structure of *KMT2B* (based on NCBI Reference Sequence: NM_014727.2) is shown indicating the location of the 7 frameshift insertions and deletions (blue, above gene), 2 stop-gain mutations (dark red, above gene), 1 splice site variant (purple, below gene) and 7 missense changes (in green, below gene). (**c**) Alignment of KMT2B amino acid sequences from seven different species, the human paralog KMT2A (another member of the MLL protein family) and the human PHF6 protein used to model the PHD-like domain. Gly1652 (in red) is highly conserved in all listed amino acid sequences, while the Phe1662 residue (in red) is either conserved or tolerates replacement by the similar amino acid, Tyr without predicted functional effect (**Supplementary Fig. 10**). (**d-g**) Alignment of KMT2B amino acid sequences from seven different species and the human paralog KMT2A. (**d**) Arg1705 (in red) is conserved to zebrafish and in human KMT2A. (**e**) Arg1762 is fully conserved throughout species. (**f**) Leu1781 (in red) is conserved in all listed mammalian homologs of KMT2B. (**g**) Arg2517 (in red) is conserved to zebrafish and in human KMT2A. (**h**) Alignment of KMT2B amino acid sequences from seven different species, the human paralog KMT2A and SET domain containing proteins (human SETD1A/SETD1B, yeast Set1, *Dictyostelium discoideum* Set1. Ile2674 (in red) is highly conserved in all listed amino acid sequences.

Residues matching human KMT2B (grey), not matching (white), amino acids conserved in all representative sequences (dark grey). ***** positions of fully conserved residues; **:**

742 conservation between groups of strongly similar properties and **.** conservation between
743 groups of weakly similar properties.

744 **Figure 2**

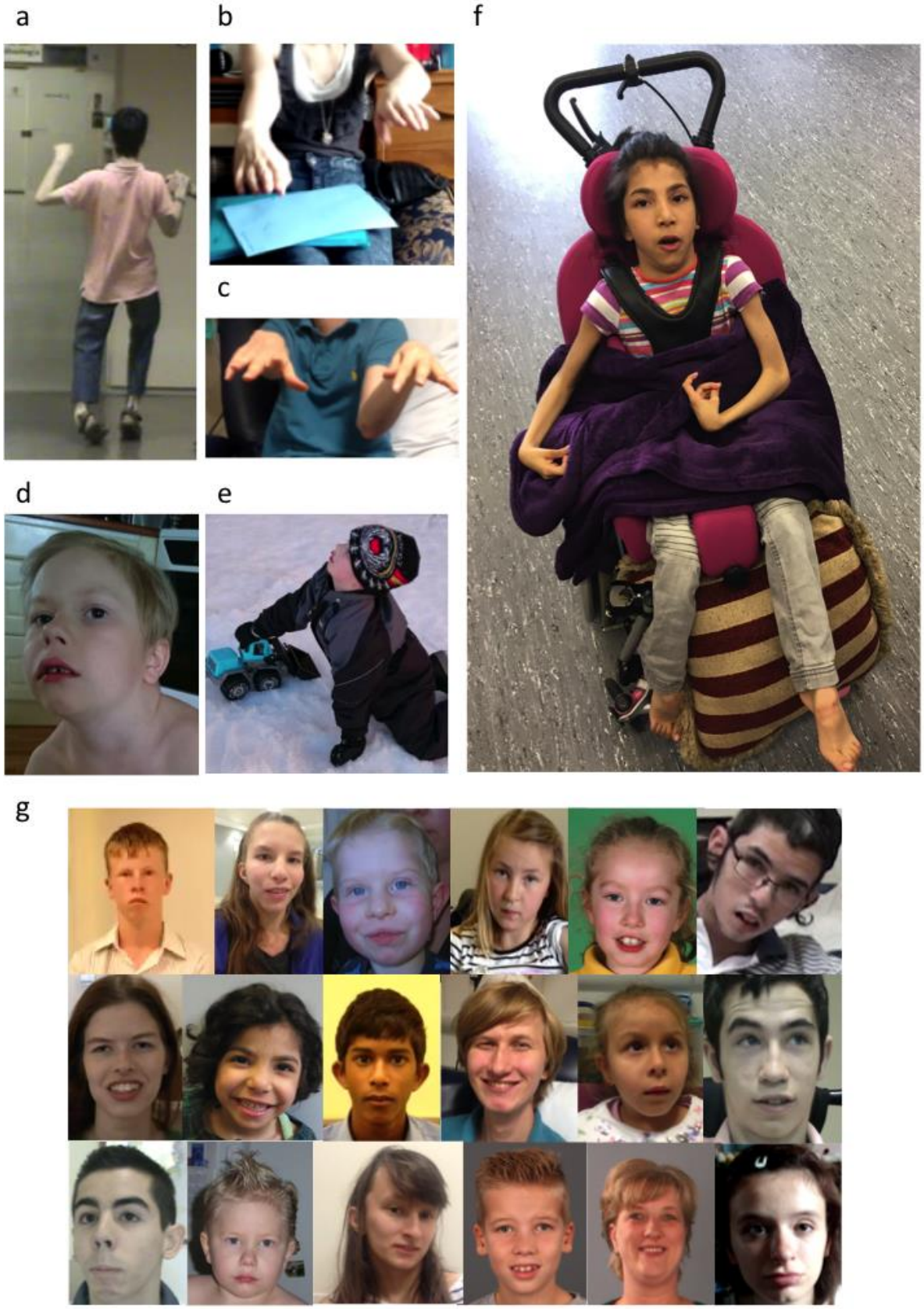
a
b
c
d
e
f
g

Figure 2:

Clinical Features of Patients with *KMT2B* Mutations

(**a**) Patient 17, age 13 years, evidence of gait disturbance with dystonic posturing of the four limbs. (**b**) Patient 27, age 19 years and (**c**) Patient 14, age 18 years both showing bilateral upper limb dystonic posturing. (**d, e**) Patient 23, age 8 years with retrocollis. (**f**) Patient 12, age 6 years, generalized dystonia, with jaw-opening dystonia and 4-limb posturing. (**g**) Montage of patient faces: Top row (left to right) Patients 1, 2, 3, 4, 8, 9; Middle row (left to right) Patients 11, 12, 13, 14, 16, 17 and Bottom row (left to right) Patients 21, 23, 25, 26a, 26b, 27. Facial elongation, broad nasal base and bulbous nasal tip, particular evident in Patients 1, 2, 4, 9, 11, 12, 14, 17, 23, 25, 26a, 26b, 27.

Figure 3

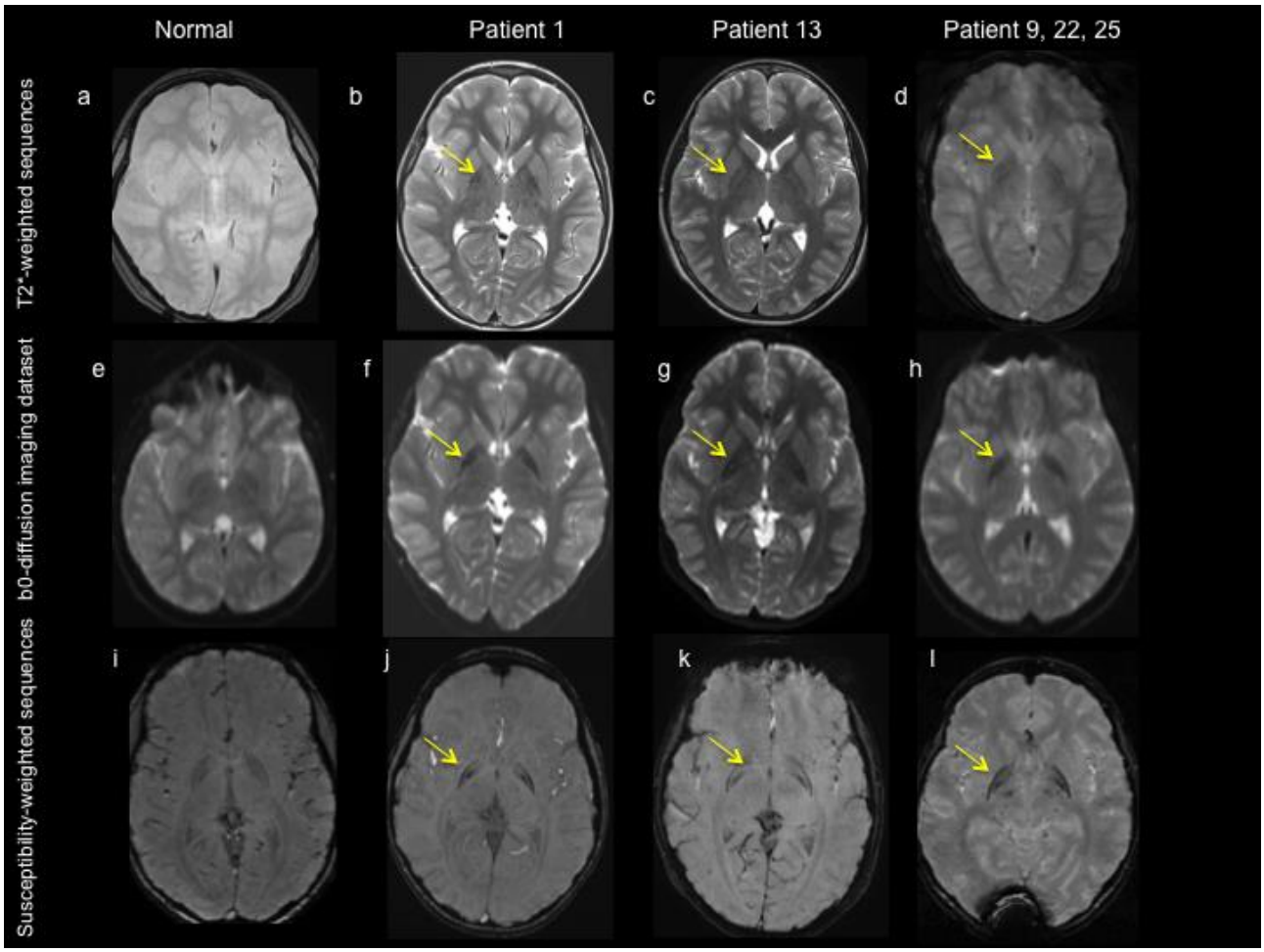

Figure 3:

Radiological Features in KMT2B-patients

Magnetic resonance imaging (MRI) with T2*-weighted sequences (**a-d**), diffusion- imaging datasets with b-value of zero (**e-h**) and susceptibility weighted sequences (**i-l**). Abnormal findings indicated by yellow arrows. (**a,e,i**) Representative MRI from control subjects for T2*-weighted sequences (**a**: age 10y2m), diffusion-weighted sequences (**e**: age 10y4m) and susceptibility weighted sequences (**i**: age 10y8m) indicating normal appearances of basal ganglia on all three sequences. (**b,f,j**) Patient 1, age 9y5m, (**c,g,k**) Patient 13, age 11y3m, (**d**) Patient 9, age 15y1m, (**h**) Patient 22 age 13y1m and (**l**) Patient 25, age 16y -

770 all show evidence of bilateral subtle hypointensity of the globus pallidus with hypointense
771 lateral streak of globus pallidus externa.

772 **Figure 4**

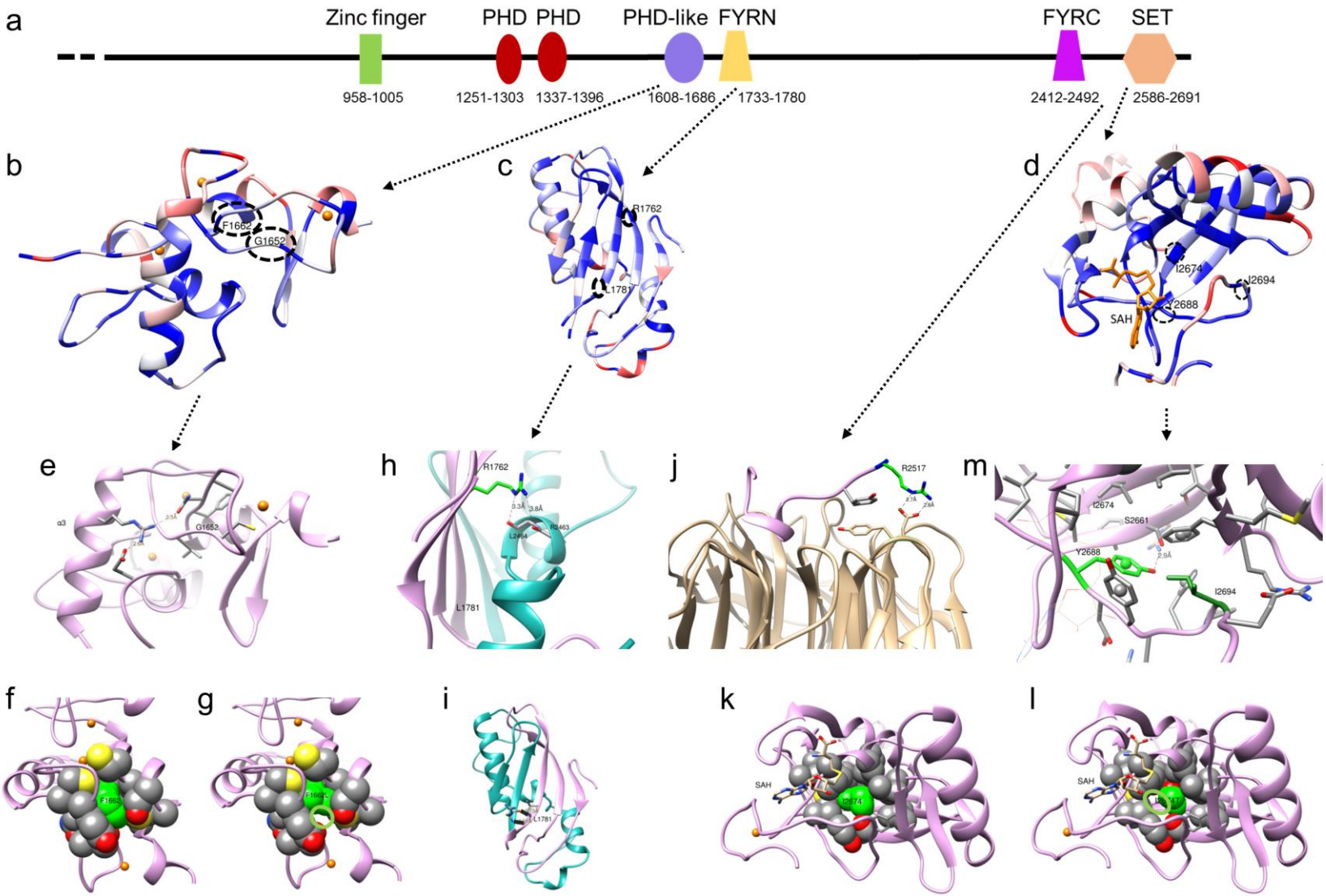

773

Figure 4:

Homology Modelling of KMT2B Protein Structure

(**a**) Schematic of domain architecture of KMT2B. (**b-d**) The degree of amino conservation is displayed in the structural models for the different domains. Red to blue indicates increasing conservation. (**b**) Model of PHD-like domain shows the mutation sites Gly1652 and Phe1662 (**c**) Model of the FYRN domain presents the position and conservation of Arg1762 and Leu1781. (**d**) Model of the SET methyltransferase domain indicates the position and conservation of Ile2674, Tyr2688 and Ile2694. (**e**) Location of Gly1652 in the PHD-like domain model and the hydrogen bond network in the vicinity are shown. Helix α3 is also indicated. (**f**) Hydrophobic packing involving Phe1662 (green) is displayed. (**g**) Change to leucine (green) at position 1662 is predicted to cause loss of contact within the hydrophobic core. Residue side chains are presented as spheres highlighting van der Waals contacts. (**h**) Interactions involving Arg1762 (green) from FYRN with Arg2463 and Leu2464 of FYRC. The hydrogen bond interactions are highlighted. (**i**) Leu1781 shown at the interface of FYRN (pink)/FYRC (blue) domains. The backbone hydrogen bonds stabilizing the sheet structure are highlighted. (**j**) Interactions involving Arg2517 (green) and WDR5 (brown). The salt bridge interaction between Arg2517 of KMT2B and Asp172 of WDR5 is highlighted. (**k**) Location and contacts involving Ile2674 (green) in the hydrophobic core of the SET domain are exhibits. SAH is displayed in light brown. (**l**) Conversion to threonine (green) at position 2674 is predicted to result in loss of contacts in the core. (**m**) Interactions involving Tyr2688 (light green) and Ile2694 (dark green) in the core of the SET domain. The hydrogen bond between Tyr2688 and Ser2661 is highlighted.

Figure 5

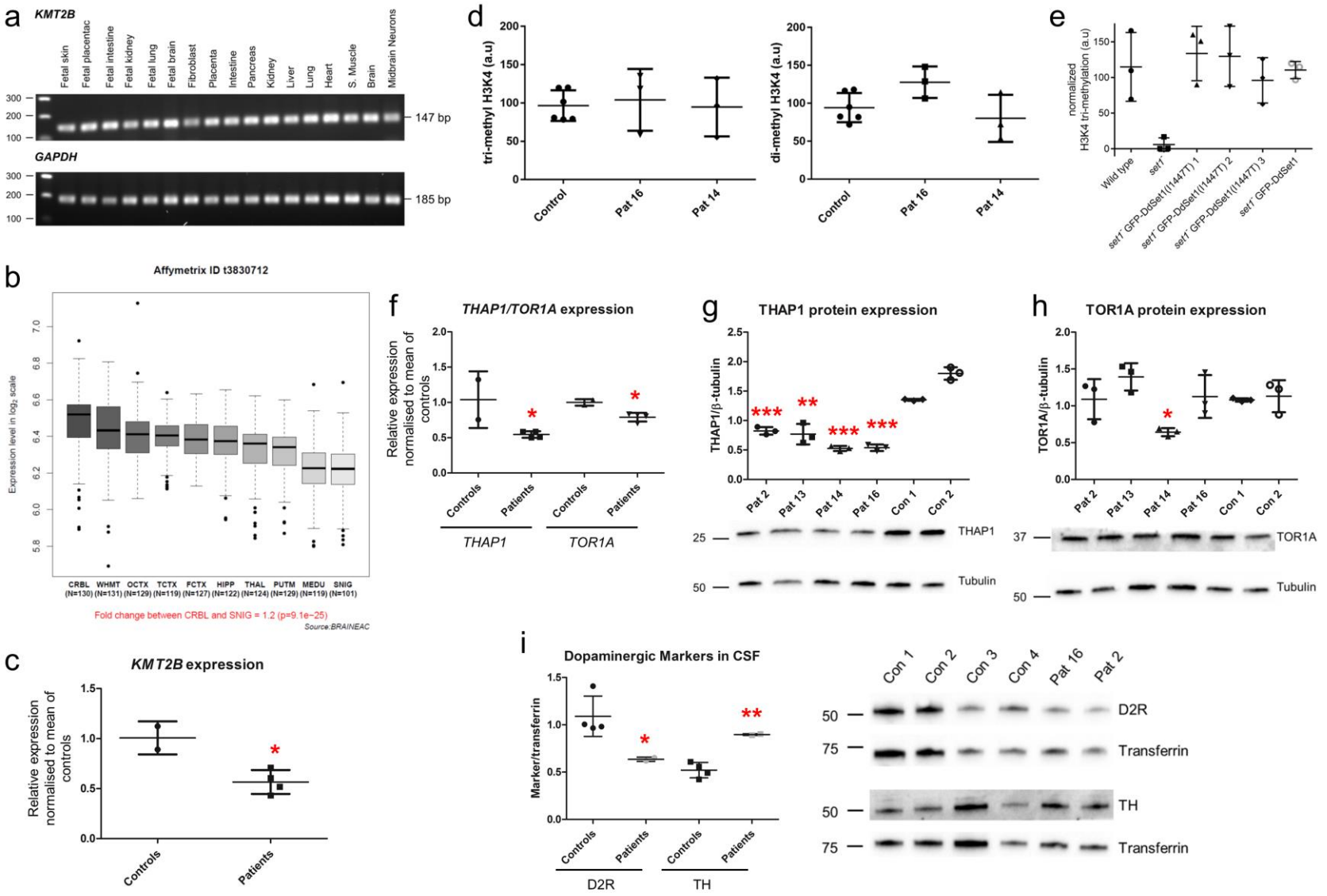
a
KMT2B
Fetal skin
Fetal placentac
Fetal intestine
Fetal kidney
Fetal lung
Fetal brain
Fibroblast
Placenta
Intestine
Pancreas
Kidney
Liver
Lung
Heart
S. Muscle
Brain
Midbrain Neurons
300
200
100
147 bp
GAPDH
185 bp
b
Affymetrix ID t3830712
Expression level in log2 scale
CRBL (N=130)
WHMT (N=131)
OCTX (N=129)
TCTX (N=119)
FCTX (N=127)
HIPP (N=122)
THAL (N=124)
PUTM (N=129)
MEDU (N=119)
SNIG (N=101)
Fold change between CRBL and SNIG = 1.2 (p=9.1e−25)
Source:BRAINEAC
c
KMT2B expression
Relative expression normalised to mean of controls
Controls
Patients
d
tri-methyl H3K4 (a.u)
di-methyl H3K4 (a.u)
Control
Pat 16
Pat 14
e
normalized H3K4 tri-methylation (a.u)
Wild type
set1-
set1- GFP-DdSet1(I1447T) 1
set1- GFP-DdSet1(I1447T) 2
set1- GFP-DdSet1(I1447T) 3
set1- GFP-DdSet1
f
THAP1/TOR1A expression
Relative expression normalised to mean of controls
Controls
Patients
THAP1
TOR1A
g
THAP1 protein expression
THAP1/β-tubulin
Pat 2
Pat 13
Pat 14
Pat 16
Con 1
Con 2
THAP1
Tubulin
h
TOR1A protein expression
TOR1A/β-tubulin
TOR1A
Tubulin
i
Dopaminergic Markers in CSF
Marker/transferrin
D2R
TH
Con 1
Con 2
Con 3
Con 4
Pat 16
Pat 2
Transferrin

Figure 5:

Functional Investigation of the Downstream Effects of Mutations in *KMT2B*

(**a**) PCR analysis of human fetal and adult cDNA for expression of *KMT2B. KMT2B* is widely expressed in a range of human tissues, including fibroblasts, brain tissue and midbrain dopaminergic neurons. (**b**) Box plots of *KMT2B* mRNA expression levels in 10 adult brain regions (source: BRAINEAC; http://www.braineac.org/). The expression levels are based on exon array experiments as previously described and are plotted on a log2 scale (y axis)[49]. This plot shows that *KMT2B* is ubiquitously expressed across all 10 brain regions analyzed, with expression higher in the cerebellum than in any other region. Putamen (PUTM), frontal cortex (FCTX), temporal cortex (TCTX), occipital cortex (OCTX). hippocampus (HIPP), substantia nigra (SNIG), medulla (specifically inferior olivary nucleus, MEDU), intralobular white matter (WHMT), thalamus (THAL), and cerebellar cortex (CRBL). "N" indicates the number of brain samples analyzed to generate the results for each brain region. Whiskers extend from the box to 1.53 the interquartile range. (**c**) Quantitative RT-PCR indicates that patients with *KMT2B* mutations (n=4) have significantly decreased fibroblast mRNA levels of *KMT2B* when compared to controls (Controls = 1.01±0.16SD, n=3 technical replicates of 2 biological samples; Patients = 0.57±0.12SD, n=3 technical replicates of 4 biological samples; two-tailed unpaired t-test, p-value 0.0182). (**d**) Quantification of immunoblotting of tri-methyl H3K4 (left) and di-methyl H3K4 (right) in histones extracted from patient-derived fibroblasts (Patient 14 and 16), and two control fibroblast cell lines. Methylation values are normalized to pan-histone H3 levels. Individual data-points are plotted with center bar showing mean and error bars showing standard deviation. Differences between control and patient-derived samples are not significant (H3K4me3: Controls = 96.63±19.98SD; Patient 16 = 104.1±40.31SD; Patient 14 = 94.75±38.36SD; p=0.62; H3K4me2: Controls = 94.33±19.25SD; Patient 16 = 127.8±20.79SD; Patient 14 = 80.23±31.09SD; p=0.07). n=3 fibroblast samples (technical

825 replicates). (**e**) Quantification of immunoblotting of tri-methyl H3K4 in *Dictyostelium* cell
826 lysates. Tri-methyl H3K4 intensity values are normalized against levels of total histone H3.
827 H3K4 tri-methylation is impaired in set1- cells compared to wild type. Expression of GFP-
828 DdSet1 or GFP-DdSet1(Ile1447Thr) in set1- cells rescues levels of H3K4Me3. Individual
829 data-points are plotted with center bar showing mean and error bars showing standard
830 deviation (Wild type = 115±48.25SD; set1- = 5.94±9.37SD; set1- GFP-DdSet1(I1447T) 1 =
831 133.7±38.11SD; set1- GFP-DdSet1(I1447T) 2 = 129.8±42.34SD; set1- GFP-
832 DdSet1(I1447T) 3 = 96.07±31.82SD; set1- GFP-DdSet1 = 110.5±12.02SD). n=3 samples
833 (technical replicates). (**f**) Quantitative RT-PCR of *THAP1* and *TOR1A*, indicates that
834 patients have a reduction of *THAP1,* and to a lesser extent of *TOR1A* transcripts in
835 comparison to controls (*THAP1:* Controls = 1.04±0.40SD, n=3 technical replicates of 2
836 biological samples; Patients = 0.55±0.05SD, n=3 technical replicates of 4 biological
837 samples; two-tailed unpaired t-test, p-value 0.0498; *TOR1A:* Controls = 1.00±0.05SD, n=3
838 technical replicates of 2 biological samples; Patients = 0.79±0.06SD, n=3 technical
839 replicates of 4 biological samples; two-tailed unpaired t-test, p-value 0.0140). (**g**)
840 Immunoblotting studies in fibroblasts indicate a significant reduction in THAP1 for Patient
841 2, 13, 14 and 16 when compared to controls (Control 1 = 1.34±0.02SD; Control 2 = 1.80±
842 0.11SD; Patient 2 = 0.83±0.06SD; Patient 13 = 0.77±0.17SD; Patient 14 = 0.53±0.04SD;
843 Patient 16 = 0.54±0.06SD; Kruskal-Wallis test, p-value 0.0078). n=3 fibroblast protein
844 samples (technical replicates). (**h**) Immunoblotting studies in fibroblasts indicate a
845 statistically reduced level of TOR1A in Patient 14 when compared to controls (Control 1 =
846 1.08±0.02SD; Control 2 = 1.13± 0.22SD; Patient 14 = 0.64±0.05SD; two-tailed unpaired t-
847 test, p-value 0.0196), but not for Patient 2, 13 and 16 (Patient 2 = 1.09±0.27SD; Patient 13
848 = 1.39±0.18SD; Patient 16 = 1.13±0.29SD; Kruskal-Wallis test, p-value 0.0812). n=3
849 fibroblast protein samples (technical replicates). (**i**) CSF immunoblotting studies on Patient

2 and 16 show markedly reduced levels of D2R and increased levels of TH when compared to control CSF (D2R: Controls = 1.09±0.21SD, n=4 control CSF samples (biological replicates); Patients = 0.64±0.02SD, n=2 patient CSF samples (biological replicates); two-tailed unpaired t-test, p-value 0.0471; TH: Controls = 0.52±0.08SD, n=4 control CSF samples (biological replicates); Patients = 0.90±0.01SD, n=2 patient CSF samples (biological replicates); two-tailed unpaired t-test, p-value 0.0036).

Table 1a: *KMT2B* Mutations and Evolution of Motor Phenotype in KMT2B-dystonia

Pat	Age (y) Sex M/F	*KMT2B* mutation[1]	Symptoms at presentation: Body distribution & motor features	Onset of dystonia (y)	Bilateral LL involve-ment (y)	Bilateral UL involve-ment (y)	Onset of cranial, cervical, laryngeal dystonia (y)	Symptoms of cranial, cervical, laryngeal dystonia	Trial of medication and clinical response	Deep brain stimulation (DBS)
1	14 M	Deletion: Chr19: 35,608,666- 36,233,508	RLL Right foot posturing Gait disturbance	4	6	6-11	5	Dysarthria Dysphonia Swallowing difficulties	L-dopa trial – no benefit	No
2	14 F	Deletion: Chr19: 35,197,252- 38,140,100	Bilateral LL Limping Gait disturbance	7	7	8-11	8	Dysarthria Dysphonia Drooling	L-dopa trial – no benefit BLF – no benefit	No
3	9 M	Deletion: Chr19: 34,697,740- 37,084,510	RLL Right foot posturing Gait disturbance	2.5	3	6-7	4	Dysarthria Dysphonia Swallowing difficulties Drooling	GBP – some reduction in tone	No
4	11 F	Deletion: Chr19: 36,191,100- 36,376,860	LLL Left toe walking Gait disturbance	4	8	9-12 m	5	Dysarthria Dysphonia Swallowing difficulties Drooling	L-dopa trial– minimal benefit THP – minimal benefit	Planned for 2016
5	20 M	Deletion: Chr19: 31,725,360- 36,229,548	Developmental delay Gait disturbance	Present but age of onset not known	Present but age of onset not known	Present but age of onset not known	Not known	Nasal voice	None	No
6	10 F	Deletion: Chr19: 35,017,972- 36,307,788	RLL Right foot inversion	2.5	4	4	4-7	Dysarthria/Anarthria Jaw-opening dystonia Swallowing difficulties NGF 6y PEG 8y Torticollis Severe retrocollis	L-dopa trial – no benefit THP – no benefit	Inserted age 7y Sustained excellent clinical benefits 3y post-DBS, marked improvement in torticollis, retrocollis, manual abilities and left leg dystonia. Loss of efficacy when 'DBS off' for almost a year and functional recovery when switched on again.
7	21 M	Deletion: Chr19: 35,414,997- 37,579,142	RLL Right foot dragging Gait disturbance	7	7-8	13	13	Dysarthria Dysphonia Swallowing difficulties	L-dopa trial – no benefit BLF – no benefit	No

Pat	Age (y) Sex M/F	*KMT2B* mutation[1]	Symptoms at presentation: Body distribution & motor features	Onset of dystonia (y)	Bilateral LL involve-ment (y)	Bilateral UL involve-ment (y)	Onset of cranial, cervical, laryngeal dystonia (y)	Symptoms of cranial, cervical, laryngeal dystonia	Trial of medication and clinical response	Deep brain stimulation (DBS)
8	17 F	Deletion: Chr19: 35,414,997-37,579,142	RLL Right foot posturing	4	6	4-12	2.5	Dysarthria Dysphonia Drooling Torticollis	L-dopa trial – no benefit	Inserted age 10y Good response over 6 years, particularly evident after replacement of faulty right DBS lead
9	14 M	Deletion: Chr19: 35,967,904-37,928,373	Bilateral LL Gait disturbance	4	4	9-13	9	Dysarthria Dysphonia	L-dopa trial – possible initial benefit but not sustained	Inserted age 14y Very good clinical response at 4m post DBS with restoration of independent ambulation
10	7 F	Deletion: Chr19: 35,794,775-38,765,822	Bilateral LL Intermittent toe walking Gait disturbance	4	4	-	-	-	None	No
11	25 F	c.399_400insT p.Pro134Serfs*24	RUL Right Hand Cramps and Posturing	6	12	12	14[2]	Anarthria Orolingual dystonia Tongue thrusting Swallowing difficulties PEG	L-dopa trial – poorly tolerated, no benefit	Being considered
12	6 F	c.1690C>T p.Arg564*	Bilateral LL Toe walking	4	5	6	5	Dysarthria Swallowing difficulties	L-dopa trial – no benefit	No
13	11 M	c.3026_3027del p.Glu1009Glyfs*9	Bilateral UL Posturing, tremor Difficulty handwriting	8	9-10	8	9	Dysarthria Dysphonia	L-dopa trial – no benefit	No
14	18 M	c.3143_3149del p.Gly1048Glufs*132	Bilateral UL Posturing of hands Myoclonic jerks	8	13	8	13	Dysarthria Dysphonia Swallowing difficulties	L-dopa trial – no benefit	No
15	20 F	c.4545C>A p.Tyr1515*	Bilateral LL Toe Walking Clumsy	2	9	9	8.5	Dysarthria Dysphonia Oromandibular dystonia Swallowing difficulties PEG 18y	Moderate responses to (and currently taking) THP CLZ L-dopa BLF	No

360

Pat	Age (y) Sex M/F	*KMT2B* mutation[1]	Symptoms at presentation: Body distribution & motor features	Onset of dystonia (y)	Bilateral LL involve-ment (y)	Bilateral UL involve-ment (y)	Onset of cranial, cervical, laryngeal dystonia (y)	Symptoms of cranial, cervical, laryngeal dystonia	Trial of medication and clinical response	Deep brain stimulation (DBS)
16	6 F	c.4688del p.Ala1563Aspfs*83	Bilateral LL Increasing falls Gait disturbance	3	3	5	6	Dysarthria Dysphonia	L-dopa trial – no benefit THP – initial benefit, not sustained	No
17	17 M	c.6515_6518delins p.Val2172Alafs*11.	Bilateral LL Toe walking Gait disturbance	1	1	8	12	Dysarthria Dysphonia Swallowing difficulties	L-dopa trial – no benefit TBZ – no benefit BLF and THP – mild benefit	Inserted age 16y Very good clinical response 4m post-DBS with restoration of independent ambulation
18	20 F	c.8061del p.Tyr2688Thrfs*50	Clumsy movements Difficulties with speech articulation	1	-	-	Infancy	Dysarthria Dysphonia Swallowing and chewing difficulties	No	No
19	28 M	c.8076del p.Ile2694Serfs*44	Bilateral LL Toe walking Severe speech delay	2	3	4 (L>R)	7	Anarthria Jaw opening dystonia Tongue protrusion Swallowing difficulties PEG 8y L torticollis,R laterocollis	L-dopa trial – no benefit THP and TBZ reduced tongue protrusion	Inserted age 27y Improvement of jaw opening dystonia and tongue protrusion
20	40 M	c.3528+2T>A	LLL Gait disturbance L foot dragging Clumsiness	4	5	8	10	Severe dysarthria Dysphonia L Torticollis	L-dopa trial – no benefit TBZ, THP, SUL – no benefit	Inserted age 32y – no benefit. Electrode replaced in 2009 with sustained improvement in foot posture but only transient benefit to cervical, UL and LL dystonia.
21	18 M	c.4955G>A p.Gly1652Asp	RLL Right leg posturing	6	8	12	5	Dysarthria Dysphonia Swallowing difficulties	L-dopa trial – no benefit THP – not tolerated	Inserted age 15y Sustained clinical benefit 3y post-DBS, improved dystonia and independent walking
22	20 F	c.4986C>A p.Phe1662Leu	RLL Right foot posturing Abnormal gait	5	8	5-13	5-6	Dysarthria Dysphonia Swallowing difficulties Torticollis	L-dopa trial – no benefit BLF – no benefit THP – low dose, mild benefit BTX neck – reduction in pain but no functional	Inserted age 20y Very good clinical response 9m post DBS with improved dystonia and independent walking

									benefit	
Pat	**Age (y) Sex M/F**	***KMT2B* mutation[1]**	**Symptoms at presentation: Body distribution & motor features**	**Onset of dystonia (y)**	**Bilateral LL involve-ment (y)**	**Bilateral UL involve-ment (y)**	**Onset of cranial, cervical, laryngeal dystonia (y)**	**Symptoms of cranial, cervical, laryngeal dystonia**	**Trial of medication and clinical response**	**Deep brain stimulation (DBS)**
23	8 M	c.5114G>A p.Arg1705Gln	Bilateral LL Toe-walking	3	3	6	6.5	Dysarthria Torticollis	L-dopa trial – no benefit CLZ, THP, IT BLF – some benefit	Inserted age 7y with considerable benefit
24	27 F	c.5284C>T p.Arg1762Cys	LLL Tiptoe walking and in-turning of L foot	6	6	7	7	Dysarthria Anarthria from 14-15y Reduced tongue movements Swallowing preserved	L-dopa trial – no benefit THP- no benefit	No
25	19 F	c.5342T>C p.Leu1781Pro	RLL Right foot posturing Gait disturbance	8	12	13	10	Dysarthria Dysphonia Swallowing difficulties Torticollis	L-dopa trial – no benefit LVT – mild benefit	Inserted age 19y Very good clinical response 4m post-DBS with improved dystonia and ambulation[3]
26a	8 M	c.7549C>T p.Arg2517Trp	Delayed speech Delayed motor development	-	-	-	8	Severe paroxysmal retrocollis and jaw dystonia	-	No
26b	46 F	c.7549C>T p.Arg2517Trp	Bilateral UL UL posturing Torticollis Inability to walk long distances and run	23	26	23	23	Dysphonia Torticollis	None	No
27	19 F	c.8021T>C p.Ile2674Thr	RUL Posturing, tremor Difficulty handwriting Myoclonic jerks	9	11-13	10	9-10	Dysphonia	L-dopa trial – no benefit THP – no benefit LVT – no benefit CBZ – initial benefit, not sustained CLZ – not tolerated	No

BLF: baclofen; BTX: botulinum toxin; CLZ: clonazepam; GBP: gabapentin; IT: intrathecal; LL: lower limbs; LLL: left lower limb; LVT: levetiracetam; m: months; NGF: nasogastric feeding; Pat: patient; PEG: percutaneous endoscopic gastrostomy; RLL: right lower limb; RUL: right upper limb; SUL: sulpiride; UL: upper limbs; TBZ: tetrabenzine; THP: trihexyphenidyl; y: years

[1] based on NCBI Reference Sequence: NM_014727.2

[2] onset shortly after being fitted with orthodontic braces

[3] had undergone 2 posterior cranial fossa explorations and palatal surgery before DBS

867 **Table 1b: Additional Clinical Features in KMT2B-patients**

Patient	*KMT2B* mutation	Number of genes in microdeletion	Intellectual disability	Dysmorphic features	Additional neurological features	Psychiatric features	Abnormal skin features	Other systemic manifestations
1	Deletion: Chr19: 35,608,666-36,233,508	38	Mild	Elongated face	Not reported	Not reported	Not reported	Not reported
2	Deletion: Chr19: 35,197,252- 38,140,100	124	No	Elongated face Bulbous nasal tip	Not reported	Not reported	Not reported	Not reported
3	Deletion: Chr19: 34,697,740 -37,084,510	109	Moderate	Elongated face	Not reported	Not reported	Cutis aplasia(1)	Retinal dystrophy
4	Deletion: Chr19: 36,191,100-36,376,860	14	V mild - subtle memory problems	Elongated face Broad nasal bridge Bulbous nasal tip	Not reported	Prone to anxiety(2)	Not reported	Not reported
5	Deletion: Chr19: 31,725,360-36,229,548	110	Moderate	Sparse hair Blepharophimosis Absent eyelashes of lower eyelids Low set, posteriorly rotated ears Epicanthic folds Narrow nasal bridge, ridge and point Largely bifid tongue Micrognathia Teeth overcrowding Finger contractures 5th finger clinodactyly Toe over-riding Dysplastic toenails	Microcephaly	Not reported	Occipital cutis aplasia	Small echogenic kidneys with low GFR, required renal transplant at 17 years
6	Deletion: Chr19: 35,017,97-36,307,788	69	No	Not reported	Microcephaly	Not reported	Not reported	Not reported
7	Deletion: Chr19: 35,414,997-37,579,142	99	Mild	Elongated face	Absence seizures	Not reported	Not reported	Absent right testis
8	Deletion: Chr19: 35,414,997-37,579,142	99	Mild	5th finger clinodactyly	Not reported	Not reported	Ectodermal dysplasia	Not reported
9	Deletion: Chr19: 35,967,904-37,928,373	79	Mild	Elongated face	Strabismus	Not reported	Not reported	Cleft palate
10	Deletion: Chr19: 35,794,775-38,765,822	111	Moderate	Not reported	Strabismus	Not reported	Not reported	Short stature Bronchiectasis

868

Patient	*KMT2B* mutation	Number of genes in microdeletion	Intellectual disability	Dysmorphic features	Additional neurological features	Psychiatric features	Abnormal skin features	Other systemic manifestations
11	c.399_400insT p.Pro134Serfs*24	-	No	Bulbous nasal tip	Not reported	Not reported	Not reported	Not reported
12	c.1690C>T p.Arg564*	-	Moderate	Elongated face Bulbous nasal tip, short nasal root, Hypertelorism, large mouth with full lower lip	Epilepsy	Not reported	Not reported	Not reported
13	c.3026_3027del p.Glu1009Glyfs*9	-	V mild - difficulties with attention	Elongated face	Not reported	Not reported	Not reported	Not reported
14	c.3143_3149del p.Gly1048Glufs*132	-	No	Elongated face Bulbous nasal tip	Not reported	Not reported	Not reported	Not reported
15	c.4545C>A p.Tyr1515*	-	No	Elongated face Bulbous nasal tip	Not reported	Not reported	Not reported	Not reported
16	c.4688del p.Ala1563Aspfs*83	-	No	Elongated face	Not reported	Not reported	Not reported	Not reported
17	c.6515_6518delins p.Val2172Alafs*11.	-	No	Elongated face	Not reported	Not reported	Phimosos	Short stature
18	c.8061del p.Tyr2688Thrfs*50	-	Mild	Micrognathia Atrophic tongue Bulbous nasal tip 5^{th} finger clinodacytly	Not reported	Not reported	Not reported	Not reported
19	c.8076del p.Ile2694Serfs*44	-	No	Short stature	Delay in saccade initiation and hypometric vertical saccades	ADHD[3] with no response to Ritalin	Not reported	Not reported
20	c.3528+2T>A	-	Moderate 6y- verbal IQ 74 Performance IQ 87 No cognitive decline	Not reported	Not reported	Not reported	Not reported	Not reported
21	c.4955G>A p.Gly1652Asp	-	Mild	Elongated face	Not reported	Not reported	Not reported	Short stature Hypertrichosis
22	c.4986C>A p.Phe1662Leu	-	No	Elongated face Bulbous nasal tip	Not reported	Not reported	Not reported	Not reported

869

Patient	*KMT2B* mutation	Number of genes in microdeletion	Intellectual disability	Dysmorphic features	Additional neurological features	Psychiatric features	Abnormal skin features	Other systemic manifestations
23	c.5114G>A p.Arg1705Gln	-	Mild-moderate 6y WISC-IV 50-60	Elongated face Bulbous nasal tip Broad philtrum, Upslanted eyes, epicanthus, low-set ears, periorbital fullness, gap between front teeth	Spasticity in lower limbs from 6y	Not reported	Ichtyotic skin lesions with criss-cross pattern under the feet and at knees, broad scarring after operation	Episodic vomiting
24	c.5284C>T p.Arg1762Cys	-	No	Short stature	Oculomotor apraxia with difficulty initiating saccades. Mild spasticity	No	Not reported	Not reported
25	c.5342T>C p.Leu1781Pro	-	No	Elongated face Bulbous nasal tip	Not reported	Not reported	Not reported	Not reported
26a	c.7549C>T p.Arg2517Trp	-	No	Bulbous nasal tip	None	ADHD[3] Currently on methyphenidate, oxazepam, risperidone	Not reported	Not reported
26b	c.7549C>T p.Arg2517Trp	-	No	Bulbous nasal tip	Idiopathic intracranial hypertension – on acetazolamide	None	Not reported	Not reported
27	c.8021T>C p.Ile2674Thr	-	V subtle mild learning difficulties	Bulbous nasal tip	Not reported	Anxiety Self-harm behavior Depression Obsessive-compulsive traits[4]	Not reported	Not reported

[1] Supplementary Figure 3c
[2] Identified on formal psychology review
[3] Diagnosed by psychiatrist and under regular psychiatry review
[4] Under regular review with psychiatrist (ICD-10-CM F06.30; ICD-10-CM F42)
ADHD: attention deficit hyperactivity disorder; GFR: glomerular filtration rate; V: very; y: years